MAXIMIZING THE ENERGY PRODUCT IN $THMN_{12}$-TYPE MAGNETS THROUGH ZIRCONIUM DOPING AND TITANIUM REDUCTION

MARGARIT GJOKA[1], CHARALAMPOS SARAFIDIS[2], DIMITRIS NIARCHOS[1], GEORGE C. HADJIPANAYIS[3]

[1]Department of Materials Science, INN,

NCSR "Demokritos", Athens, Greece

[2]Department of Physics, Aristotle University, Thessaloniki, Greece

[3]Department of Chemical Engineering, Northeastern University,

Boston, MA 02115, USA

e-mail: m.gjokas@inn.demokritos.gr

Abstract

The development of high-performance permanent magnets free from critical rare-earth elements is a crucial goal for sustainable technologies like electric vehicles and wind turbines. $ThMn_{12}$-type (1:12) alloys are promising candidates due to their strong magnetic properties, high Curie temperature, and rare-earth-lean composition. The primary objective of this research was to maximize the energy product ($(BH)_{max}$, a critical performance metric for permanent magnets, in rare-earth-lean $ThMn_{12}$-type alloys. The investigation demonstrates a pathway to significantly enhance this parameter through careful compositional and processing control. A key achievement of this work is the attainment of an exceptional energy product of approximately 289 kJ/m³ in a $Sm(Fe,Co,Ti)_{12}$-based alloy with a strategically modified composition $Sm_{0.75}Zr_{0.25}Fe_{9.04}Co_{2.26}Ti_{0.7}$. The study systematically explored alloys synthesized via arc-melting, followed by high-energy ball milling (HEBM) and annealing. While Zr doping was found to slightly decrease coercivity compared to the baseline $SmFe_9Co_2Ti$ alloy, its inclusion was fundamentally vital for achieving the standout energy product in the Ti-reduced composition. Microstructural analysis confirmed that extended milling times refined the grain structure, which is essential for enhancing magnetic properties. However, the delicate balance between promoting the desired magnetic phase and preventing the formation of detrimental phases, such as Sm_2O_3 and soft

α-(FeCo), proved crucial. This work underscores that the maximization of the energy product in these promising materials is a complex interplay between elemental substitution and processing, highlighting a successful strategy for developing next-generation, cost-effective permanent magnets with reduced reliance on critical rare-earth elements.

Key words**:** *$ThMn_{12}$-type alloys, permanent magnets, high-energy ball milling, coercivity, Zirconium doping, energy product.*

Përmbledhje

Zhvillimi i magnetëve të përhershëm me performancë të lartë, pa elemente kritike të tokave të rralla, është një synim strategjik për teknologji si prodhimi i makinave elektrike dhe turbinave të erës. Përlidhjet e tipit $ThMn_{12}$ (1:12) janë kandidatë premtues për shkak të vetive të tyre të mira magnetike, temperaturës së lartë Curie dhe përmbajtjes së ulët në elemente të tokave të rralla. Objektivi kryesor i këtij studimi ishte maksimizimi i produktit të energjisë $(BH)_{max}$ në përlidhjet e tipit $ThMn_{12}$ me përmbajtje të ulët të elementeve të tokave të rralla. Studimi demonstron një rrugë për të përmirësuar ndjeshëm këtë parametër përmes një kontrolli të kujdesshëm të përbërjes dhe përpunimit. Një rezultat kyç i kësaj pune është prodhimi i materialit magnetik me një produkt energjik të kënaqshëm prej afërsisht 289 kJ/m³ në përlidhjen $Sm_{0.75}Zr_{0.25}Fe_{9.04}Co_{2.26}Ti_{0.7}$. Në këtë studim u ~~eksploruan~~ studiuan në mënyrë sistematike përlidhjet e prodhuara me shkrirje me hark elektrik, të cilat u bluan me sfera me energji të lartë (HEBM) dhe më pas u përpunuan termikisht në temperatura të larta. Ndërsa u zbulua se dopimi me Zr ulte lehtësisht forcën koericitive në krahasim me përlidhjen bazë $SmFe_9Co_2Ti$, përfshirja e tij ishte thelbësisht jetike për arritjen e një produkti të lartë energjie në përlidhjet me përbërje atomike të reduktuar të Ti. Analiza mikrostrukturore konfirmoi se kohëzgjatja optimale e bluarjes është thelbësore për përmirësimin e vetive magnetike. Megjithatë, ekuilibri delikat midis sintetizimit të fazës së dëshiruar magnetike dhe parandalimit të formimit të fazave të dëmshme, si Sm_2O_3 dhe α-(FeCo), është vendimtar. Si rezultat maksimizimi i produktit të energjisë në këto materiale premtuese është një ndërveprim kompleks për prodhimin e magnetëve të përhershëm të gjeneratës së ardhshme, me kosto efektive dhe me ulje të pranisë së elementëve kritikë të tokave të rralla.

Fjalë kyçe: *Përlidhje të tipit $ThMn_{12}$, magnetë të përhershëm, bluarje me sfera me energji të lartë, forcë koericitive, dopim me zirkon, produkti i energjisë.*

Introduction

The global push towards a green economy has created an unprecedented demand for high-performance permanent magnets, which are critical components in technologies like electric vehicle motors and wind turbine generators (Popa, 2024). For years, Neodymium-Iron-Boron (Nd-Fe-B) magnets have been the market leader due to their outstanding magnetic performance. However, the supply chain of rare-earth elements like Neodymium (Nd) and Dysprosium (Dy) is fraught with risks and environmental issues, prompting a worldwide search for alternative "gap magnets" (Podmiljšak, B. 2024). Geopolitical tensions surrounding the supply of rare-earth elements, largely controlled by a few nations, have intensified the search for alternatives. These magnets aim to bridge the performance gap between affordable ferrite magnets and high-strength Nd-Fe-B magnets by utilizing more abundant and less critical materials.

A promising class of materials for this purpose are alloys with the tetragonal $ThMn_{12}$-type crystal structure (De Mooij. & Buschow, 1988). These alloys, with the general formula $R(Fe,T)_{12}$ where **R** is a rare-earth element and **T** is a stabilizing transition metal, have a high transition metal to rare-earth ratio, making them less dependent on rare-earth elements (Ohashi, et al., 1988). Among these, Samarium (Sm)-based compounds are particularly noteworthy for their strong uniaxial magneto-crystalline anisotropy, a key requirement for a high-performance permanent magnet (Li, & Coey., 1988).

The binary $SmFe_{12}$ compound is inherently unstable and requires a third element like Titanium (Ti) for stabilization. While Ti is an effective stabilizer, it unfortunately reduces the material's magnetization. To counteract this, Cobalt (Co) is often substituted for Iron (Fe) to increase the Curie temperature and, in some cases, the anisotropy (Hirayama et al., 2017). More recently, Zirconium (Zr) doping has emerged as a promising strategy. Worldwide research has shown that substituting a small amount of Sm with Zr can help stabilize the 1:12 phase while simultaneously allowing for a reduction in the magnetization-lowering Ti content. This approach has led to remarkable improvements in intrinsic magnetic properties. For instance, Tozman et al. (2018, 2019, 2021) al. demonstrated that a $Sm_{0.8}Zr_{0.2}(Fe_{0.8}Co_{0.2})_{11.5}Ti_{0.5}$ alloy possesses intrinsic magnetic properties superior to the $Nd_2Fe_{14}B$ phase at elevated temperatures.

Similarly, Kuno et al. (2016) reported a saturation magnetization (μ_0Ms) of approximately 161 emu/g (1.58 T) in a $(Sm_{0.8}Zr_{0.2})$ $(Fe_{0.75}Co_{0.25})_{11.5}Ti_{0.5}$

alloy, rivalling that of Nd-Fe-B magnets but with a significantly higher Curie temperature (Kuno et al, 2016, Kobayashi et al., 2017). Some compositions have even achieved saturation magnetization values approaching 193 emu/g (1.9 T), the highest ever reported for this class of intermetallic compounds. While these high saturation magnetizations are a critical prerequisite for a large energy product, theoretical calculations have suggested that $(BH)_{max}$ values over 50.3 MGOe (400 kJ/m³) could be achievable in optimized Zr-doped systems (Saito, 2020). However, translating this potential into bulk materials has been hampered by the difficulty in achieving high coercivity concurrently.

The fabrication of these advanced magnets often involves nanostructuring techniques, like high-energy ball milling (HEBM) followed by an annealing process (Schultz et al., 1990., Gabay et al., 2017) or reduction-diffusion process (Dirba et al, 2021). This method refines the microstructure, leading to a fine-grained material which is crucial for maximizing coercivity, the magnet's resistance to demagnetization. Our previous work laid the groundwork by systematically investigating the synthesis and processing of these Zr-doped alloys (Gjoka et al., 2025). That study explored how milling time and annealing parameters influence the phase evolution, grain size, and key magnetic properties such as coercivity (H_c) and magnetization (σ_s).

The findings revealed a strong dependence of these properties on the processing conditions, with longer milling times and optimized annealing temperatures leading to higher coercivity. Building upon these foundational results, this study aims to further explore the potential of Zr-doped Sm(Fe, Co, Ti)$_{12}$ alloys with a specific focus on maximizing the energy product $(BH)_{max}$. The energy product is the most critical figure of merit for a permanent magnet, as it represents the total magnetic energy stored within the material. By fine-tuning the composition and processing parameters, we seek to overcome the challenge of reduced coercivity in Zr-doped samples and unlock their full potential, ultimately aiming for a new generation of high-performance permanent magnets with a reduced reliance on critical rare-earth elements.

Experimental, processing, characterization and calculation model

Four series of alloys with nominal compositions were prepared: sample A: $SmFe_9Co_2Ti$, sample B: $SmFe_{9.04}Co_{2.26}Ti_{0.7}$, sample C: $Sm_{0.75}Zr_{0.25}Fe_9Co_2Ti$ and sample D: $Sm_{0.75}Zr_{0.25}Fe_{9.04}Co_{2.26}Ti_{0.7}$. High-purity starting elements (Sm, Fe, Co, Ti, Zr) were weighed and arc-melted multiple times under a high-purity Argon atmosphere to ensure homogeneity (Reed, 1967).

A slight excess of Sm was used to compensate for potential losses due to its high vapor pressure. The as-cast ingots were crushed into a coarse powder. This powder was then subjected to high-energy ball milling (HEBM) using a SPEX-8000 mixer/mill. The milling was carried out in a hardened steel vial embedded in alcohol to prevent oxidation, with a ball-to-powder weight ratio of 10:1. Two different milling times, 4 hours and 8 hours, were investigated. The resulting milled powders were sealed in quartz tubes under vacuum and subjected to annealing for recrystallization (Schultz, et al. 1990; Suryanarayana, 2001; Gabay, 2017). The annealing was carried out at temperatures ranging from 973 K to 1173 K for durations between 15 and 90 minutes, followed by quenching in water

Phase identification and structural analysis of the as-cast, milled, and annealed powders were performed using X-ray diffraction (XRD) with Cu-K_α radiation. Microstructural characterization, including grain size and morphology analysis, was conducted using a Scanning Electron Microscope (SEM). Magnetic properties, including hysteresis (M-H) loops, were measured at room temperature using a Vibrating Sample Magnetometer (VSM) with a maximum applied field of 3 T. From these loops, the coercivity (H_c) and saturation magnetization (σ_s) were determined. Derivatives of thermomagnetic analysis (TMA) were used to determine the Curie temperatures (T_c) of the constituent phases.

To evaluate the ultimate potential of the synthesized alloys, the theoretical maximum energy product, $(BH)_{max\_ideal}$, was calculated. The energy product is a figure of merit representing the maximum energy that can be stored in a permanent magnet (Cullity et al., 2008). For an ideal magnet with a perfectly rectangular demagnetization curve (remanence Br equal to saturation polarization Js) and sufficient coercivity ($Hci \geq Js / 2\mu_0$), the theoretical maximum is given by:

$$\mathbf{(BH)_{max\_ideal} = J_s^2 / (4\mu_0)\ [1]}$$

where *Js* is the saturation magnetic polarization in Tesla (T) and μ_0 is the permeability of free space ($4\pi \times 10^{-7}$ T·m/A). Since the experimental data provides mass magnetization (σ_s in emu/g), a conversion to J_s is required.

Results and discussions

Structure and microstructure

The X-ray powder diffraction patterns of the arc-melted alloys and the corresponding Miller's indexes of 1:12 phases are shown in Figure 1. Rietveld

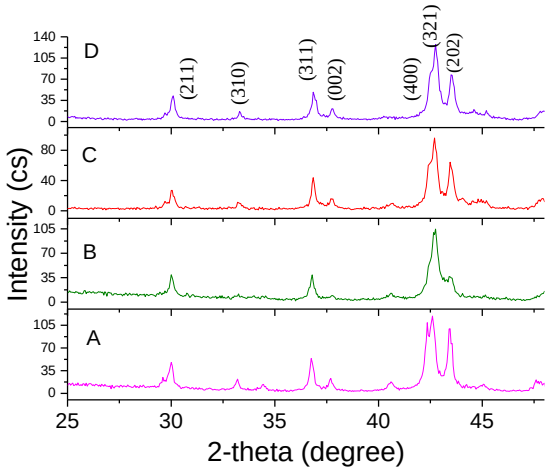

Figure 1. X-ray diffraction diagrams of powders of arc-melting alloys.

analysis of the X-ray diffraction data indicates that the as-cast alloys with a titanium atomic content of 1 (samples A and C) are predominantly single-phase. They exhibit a tetragonal 1:12 $ThMn_{12}$-type structure, belonging to the I4/mmm space group. A minor impurity of an α-(Fe, Co) phase was also detected, with a maximum content of 1.24 wt.%. When samarium (Sm) was partially substituted by zirconium (Zr) in samples B and D, a third phase emerged. This additional phase was identified as $Sm(FeCo)_2$ with a $MgZn_2$ Laves-type structure, irrespective of the titanium content (which was either 1 or 0.7).

Thermomagnetic analysis provided crucial insights into the magnetic transitions of the constituent phases, revealing their respective Curie temperatures (Tc). The first derivatives of magnetization with respect to temperature dM/dT are shown in Figure 2. For samples A and C, two distinct magnetic transitions were observed. The primary 1:12 phase exhibited a Curie temperature of 739(5) K. The minor α-(Fe, Co) phase showed a significantly higher magnetic transition at 1216(5) K. The typical Curie temperatures for α-(Fe, Co) phases are generally found within the range of 1193–1258 K, depending on the precise Fe and Co content

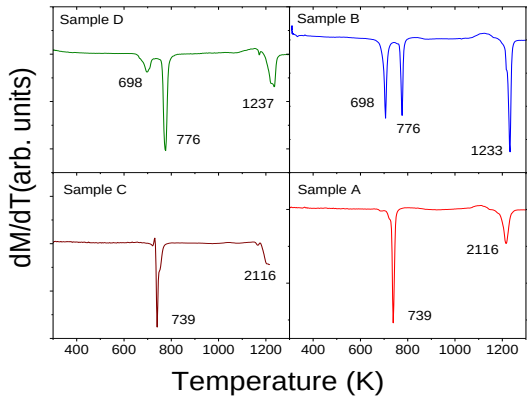

Figure 2. First derivatives of magnetization versus temperature of arc-melting alloys

In the Zr-substituted samples B and D, the newly formed $Sm(FeCo)_2$ Laves phase displayed Curie temperatures of 706(5) K and 698(5) K, respectively. These values are very close to the reported Curie temperature of 700 K for the $SmFe_2$ compound. The 1:12 phase in these samples (B and D) showed a Curie temperature of 776 K. The magnetic transitions for the minor α-(Fe, Co) phase in samples B and D were detected at 1233(5) K and 1237(5) K, respectively.

The microstructure of the alloys was further examined using scanning electron microscopy, particularly after high-energy ball milling and subsequent annealing. The grain size of the resulting powders was found to be strongly dependent on both the milling and annealing times.

For instance, a sample milled for 8 hours and then annealed at 1123 K displayed a grain size predominantly in the range of 2–6 μm. This is

considered a more optimal range for permanent magnet applications. However, the presence of grains smaller than 2 μm and larger than 6 μm was noted (Figure 3a), which can affect the overall magnetic coercivity. In contrast, this sample milled for 4 hours and annealed at the same temperature exhibited a much wider and less optimal variation in grain size, ranging from 2-4 μm up to 20 μm or even larger (Figure 3b). This broad distribution of grain sizes is not ideal for achieving high coercivity.

Following thermal treatment, the amorphous powders recrystallized into a majority 1:12 phase, accompanied by a slightly larger content of the α-(Fe,

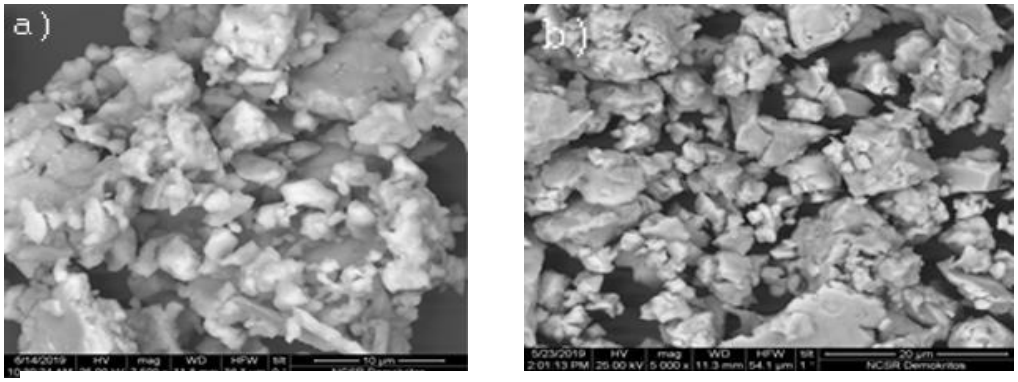

Figure 3. SEM images of $SmFe_9Co_2Ti$ milled 8 h (a) and 4 h (b) both samples annealed at 1123 K

Co) phase. A small amount of Sm_2O_3oxide was also formed during this process. The identification of multiple phases and their corresponding Curie temperatures, coupled with the characterization of the grain size distribution, offers valuable information for the further development and optimization of these materials for magnetic applications.

3.2 Magnetic Measurements

The magnetic properties of the synthesized alloys were systematically investigated by analysing their demagnetization curves. The baseline alloy, $SmFe_9Co_2Ti$ (Sample A), was milled for 4 hours and subjected to various annealing protocols to optimize its magnetic performance. Figure 4 illustrates the effect of annealing temperature on the magnetic behaviour of sample A.

The samples annealed at 973 K exhibited a relatively low coercivity of approximately 1.6 kOe. A significant improvement was observed at an annealing temperature of 1073 K, where the coercivity reached a maximum

value of 4.6 kOe after 60 minutes of annealing. Concurrently, the magnetization for this sample was measured at 117.8 emu/g.

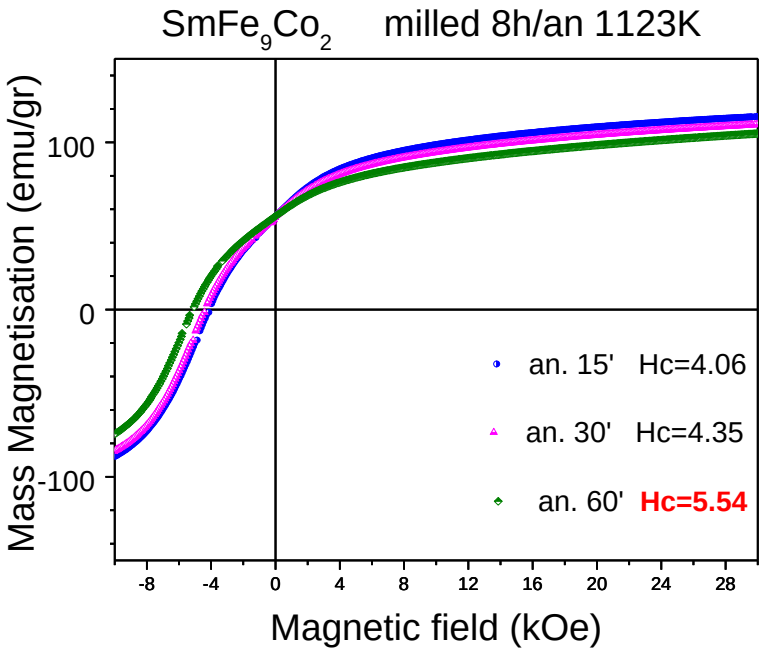

Figure 4. Demagnetization curves of $SmFe_9Co_2Ti$ powders milled for 8 hours and annealed at different time intervals at 1123K..

Further increasing the annealing temperature to 1173 K resulted in a moderate coercivity, peaking at 4.04 kOe after 30 minutes. This behaviour is attributed to the increased formation of the soft magnetic α-(Fe,Co) phase at higher temperatures. Based on the observation that coercivity increased in the 1073-1173 K range, this range was selected for further optimization of other alloy compositions.

A key trade-off between magnetic properties was identified upon modification of the baseline composition. While Sample A achieved the highest coercivity of 5.5 kOe, its saturation magnetization was relatively low at 105 emu/g. In contrast, Sample D ($Sm_{0.75}Zr_{0.25}Fe_{9.04}Co_{2.26}Ti_{0.7}$), after milling for 8h and annealing at 1123 K for just 15 minutes, exhibited a moderate coercivity of 4.05 kOe but a significantly higher saturation magnetization of approximately 120.8 emu/g. This enhanced magnetization in Sample D led to an impressive experimental energy product ($(BH)_{max}$ of 289.3 kJ/m³ (Table 1), highlighting

a successful strategy where Zr-doping and reduced Ti content effectively boost magnetization to compensate for a modest decrease in coercivity.

Prediction of Maximum Energy Product ((BH)) $_{max}$

Theoretical $(BH)_{max}$ of annealed powders was calculated for the most promising samples. The results are summarized in the Table 1. The calculations of the theoretical maximum energy product are provided in the appendix. These are theoretical maximum values assuming ideal loop squareness.

Table 1 of Calculated Theoretical $(BH)_{max}$_ideal for samples A, and D

Sample Description	σ_{3T} (emu/g)	ρ (g/cm³)	Hc (kOe)	(BH)max (kJ/m³)	(BH)max (MGOe)
A, milled 8h, ann. 1123K, 60min	105	7.76	5.5	208.6	26.2
A milled 4h, ann. 1073K, 60min	118	7.76	4.6	263.4	33.1
D, milled 8 h, ann. 1123K, 60min	125.6	7.64	2.76	289.3	36.4
D, milled 8h, ann. 1123K, 15min	120.8	7.64	4.05	267.6	33.6

Squareness of Demagnetization Curves and Challenges

The shape of the demagnetization curve, particularly its "squareness," is a critical factor for a high-performance permanent magnet. An ideal magnet exhibits a perfectly square loop in the second quadrant, which ensures the largest possible energy product for a given remanence and coercivity.[2]

Upon inspection of the experimental curves in Figure 5, it is evident that the loops are not perfectly square. They exhibit a sloped or "sheared" shape, which indicates that the magnetic reversal process is not uniform. This imperfect squareness directly reduces the achievable energy product from its theoretical maximum.

The primary challenges to improving the squareness and overall magnetic performance in this materials system are microstructural:

- **Presence of Soft Magnetic Phases:** The text explicitly notes the formation of a soft α-(Fe,Co) phase, especially at higher annealing temperatures. This phase has low coercivity and initiates magnetic reversal at lower fields, degrading the squareness and coercivity of the composite material.

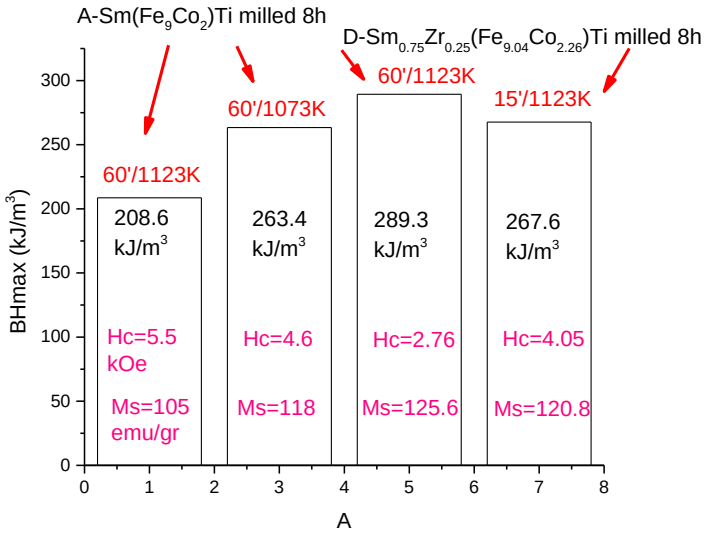

Figure 5. $(BH)_{max}$ values and corresponding magnetic properties for the best-performing samples.

- **Harmful Secondary Phases:** The introduction of zirconium, while beneficial for magnetization, was found to promote the formation of an undesirable $Sm(FeCo)_2$ Laves phase. Such secondary phases can act as nucleation sites for reverse magnetic domains, further compromising coercivity and loop shape.

- **Grain Structure and Isolation:** For optimal performance, a microstructure of fine, uniform, and magnetically isolated hard magnetic grains is required. Inhomogeneous grain growth or poor isolation between grains can lead to cooperative demagnetization, reducing both squareness and coercivity.

Overcoming these challenges requires precise control over alloy composition and processing to suppress the formation of these detrimental phases and to engineer a more ideal nanocomposite grain structure.

Conclusions

This study successfully synthesized and characterized a series of Sm(Fe, Co, Ti)$_{12}$-based alloys, demonstrating their significant potential as RE-lean permanent magnets. The investigation revealed a critical interplay between processing, composition, and magnetic properties. High-energy ball milling, particularly for an extended duration of 8 hours, was essential for achieving a fine-grained microstructure prerequisite for high coercivity.

The highest coercivity of **5.5 kOe** was achieved in the baseline $SmFe_9Co_2Ti$ alloy (Sample A), establishing a benchmark for this material system when processed via ball milling. A more promising compositional trade-off was identified in Sample D ($Sm_{0.75}Zr_{0.25}Fe_{9.04}Co_{2.26}Ti_{0.7}$), where a combination of Zr-doping and reduced Ti content yielded an outstanding experimental energy product ($(BH)_{max}$ of approximately **289 kJ/m³**. This was achieved due to a significantly enhanced saturation magnetization (~120.8 emu/g), which more than compensated for its moderate coercivity (4.05 kOe).

Theoretical calculations underscore the even greater potential of these materials, predicting ideal energy products as high as 289.3 kJ/m³ (36.4 MGOe) for compositions with high saturation magnetization. However, the analysis also highlighted that achieving these theoretical limits is currently constrained by insufficient coercivity and non-ideal squareness of the hysteresis loops. The primary challenge lies in mitigating the formation of deleterious secondary phases, such as soft α-(Fe,Co) and Sm(FeCo)$_2$ Laves phases, which degrade the magnetic properties.

Future work should be directed towards optimizing the alloy compositions, particularly the Zr/Ti ratio, and refining annealing protocols to suppress secondary phase formation. Success in engineering the microstructure to enhance coercivity and loop squareness will be crucial to unlocking the full potential of these promising Sm-Fe-Co-Ti alloys as a viable alternative to traditional rare-earth permanent magnets.

References

Cullity, B. D., Graham, C. D. (2008): “Introduction to Magnetic Materials”, first ed. IEEE Press, NJ, pp. 480- 483. ISBN: 9780471477419

De Mooij, D.B., Buschow, K.H.J., (January 1988): "Some Novel Ternary $ThMn_{12}$-Type Compounds", J. Less Common Met., 136, pp 207–215.

https://doi.org/10.1016/0022-5088(88)90424-9.

Dirba, I., Sepehri-Amin, H., Choi, I.-J., Choi, J.-H., Uh, H.-S., Kim, T.-H., Kwon, S.-J., Ohkubo, T., Hono, K., (April 2021): "$SmFe_{12}$-Based Hard Magnetic Alloys Prepared by Reduction-Diffusion Process", J. Alloy Compd., vol 861, 157993.

https://doi.org/10.1016/j.jallcom.2020.157993.

Gabay, A.M. and Hadjipanayis, G.C., (January 2017): “Mechanochemical Synthesis of Magnetically Hard Anisotropic $RFe_{10}Si_2$ Powders with Representing Combinations of Sm, Ce and Zr", J. Magn. Magn. Mater., vol. 422, pp. 43-48.

https://doi.org/10.1016/j.jmmm.2016.08.064.

Gjoka, M., Sarafidis, C., Niarchos, D., & Hadjipanayis, G. (March 2025): Effect of Annealing Conditions of High-Energy Ball-Milled $Sm(Fe, Co, Ti)_{12}$ Alloys Doped with Zr on Microstructure and Magnetic Properties, Materials, vol. 18(7), pp. 1642.

https://doi.org/10.3390/ma18071642.

Hirayama Y., Takahashi Y.K., Hirosawa S., Hono K.,(September 2017): “Intrinsic hard magnetic properties of $Sm(Fe_{1-x}Co_x)_{12}$ compound with the $ThMn_{12}$ structure”, Scripta Materialia, vol. 138, pp. 62-65. https://doi.org/10.1016/j.scriptamat.2017.05.029.

Kobayashi, K., Suzuki, S., Kuno, T., Urushibata, K., Sakuma, N., Yano, M., Shouji, T., Kato, A., Manabe, A. (February 2017), “The Stability of Newly Developed $(R,Zr)(Fe,Co)_{12-x}Ti_x$ Alloys for Permanent Magnets". J. Alloy Compd., vol. 694, pp. 914-920.

https://doi.org/10.1016/j.jallcom.2016.09.311.

Kuno T., Suzuki S., Urushibata K., Kobayashi K., 1, Sakuma N., Yano M., Kato A., and Manabe A., (February 2016): "$(Sm,Zr)(Fe,Co)_{11.0\text{-}11.5}Ti_{1.0\text{-}0.5}$ compounds as new permanent magnet materials", AIP Advances 6, 025221.

https://doi.org/10.1063/1.4943051.

Li, H.-S., Coey, J.M.D., (1991): “Magnetic Properties of Ternary Rare-Earth Transition-Metal Compounds. In Handbook of Magnetic Materials; Buschow, K.H.J., Ed.; North Holland Publishing Co.: Amsterdam, The Netherlands, Vol. 6, pp. 1-83.

Ohashi, K., Tawara, Y., Osugi, R., Shimao, M., (November 1988): Magnetic Properties of Fe-rich Rare-earth Intermetallic Compounds with a ThMn12 Structure. J. Appl. Phys. Vol. 64, pp. 5714-5716.

https://doi.org/10.1063/1.342235.

Podmiljšak, B., Saje, B., Jenuš, P., Tomše, T., Kobe, S., Žužek, K., & Šturm, S. (February 2024): "The Future of Permanent-Magnet-Based Electric Motors: How Will Rare Earths Affect Electrification? Materials", vol. 17(4), pp. 848.

https://doi.org/10.3390/ma17040848.

Popa, D.-C., & Szabó L., (November 2024): Securing Rare Earth Permanent Magnet Needs for Sustainable Energy Initiatives. Materials, 17(22), 5442.

https://doi.org/10.3390/ma17225442.

Reed, T. B. (March 1967): "Arc techniques for materials research", *Materials Research Bulletin*, vol. 2(3), pp. 349–367.

https://doi.org/10.1016/0025-5408(67)90018-9

Saito A. T., (2020): "Recent progress of $ThMn_{12}$-type hard magnetic compounds." Journal of Physics D: Applied Physics, 53.28: 283001. DOI: 10.1088/1361-6463/ab8669.

Schultz, L., Schnitzke, K., Wecker, (February 1990): "J. High coercivity in mechanically alloyed Sm-Fe-V magnets with a $ThMn_{12}$ crystal structure", Appl. Phys. Lett., vol. 56, pp. 868–870. https://doi.org/10.1063/1.102662.

Suryanarayana, C. (2001): "Mechanical alloying and milling." *Progress in Materials Science*, vol. 46(1-2), pp. 1–184.
https://doi.org/10.1016/S0079-6425(99)00010-9

Tozman, A P., Sepehri-Amin, H., Takahashi, Y.K., Hirosawa, S., Hono, K., (2018): "Intrinsic Magnetic Properties of $Sm(FeCo)_{11}Ti$ and Zr-Substituted $Sm_{1-y}Zr$ $(Fe_{0.8}Co_{0.2})_{11.5}Ti_{0.5}$ Compounds with $ThMn_{12}$ Structure toward the Development of Permanent Magnets", Acta Mater", vol 153, pp 354-363.

https://doi.org/10.1016/j.actamat.2018.05.008

Tozman, P.; Takahashi, Y.K.; Sepehri-Amin, H.; Ogawa, D.; Hirosawa, S.; Hono, K. (October 2019): "The Effect of Zr Substitution on Saturation Magnetization in $(Sm_{1-x}Zr_x)(Fe_{0.8}Co_{0.2})_{12}$ Compound with the ThMn12 Structure", Acta Mater. Vol. 178, pp. 114–1.

https://doi.org/10.1016/j.actamat.2019.08.003.

Tozman, P., Sepehri-Amin, H., Hono, K. (March 2021): "Prospects for the Development of SmFe12-Based Permanent Magnets with a ThMn12-Type Phase", Scr. Mater. 194, 113686.

https://doi.org/10.1016/j.scriptamat.2020.113686.

Appendix

Calculation the theoretical maximum energy product $(BH)_{max}$ for one of the HEBM annealed powders. The theoretical maximum energy product for a magnetic material, assuming an ideal rectangular demagnetization curve (perfect squareness with Br = Js) and sufficient coercivity ($Hci \geq Js / 2\mu_0$), is given by:

$$(BH)_{max\_ideal} = Js^2 / (4\mu_0)$$

where Js is the saturation magnetic polarization in Tesla (T); μ_0 is the permeability of free space ($4\pi \times 10^{-7}$ T·m/A). We are given magnetization M_{3T} (σ_s in emu/g, which we'll use as a proxy for saturation magnetization σ_s). We need to convert this to Js. All steps are described below.

1. Convert mass magnetization (σ_s in emu/g) to volume magnetization (Ms_vol in emu/cm³):

$$M_s\_vol\ (emu/cm^3) = \sigma_s\ (emu/g) \times \rho\ (g/cm^3)$$

where ρ is the density of the material.

2. Convert volume magnetization from emu/cm³ to A/m:

$$M_s\_vol\ (A/m) = Ms\_vol\ (emu/cm^3) \times 1000$$

3. Calculate saturation polarization Js:

$$J_s\ (T) = \mu_0 \times Ms\_vol\ (A/m)$$

$$J_s\ (T) = 4\pi \times 10^{-7}\ (T \cdot m/A) \times \sigma_s\ (emu/g) \times \rho\ (g/cm^3) \times 1000\ (A \cdot m^{-1} / emu \cdot cm^{-3})$$

$$J_s\ (T) = \sigma_s\ (emu/g) \times \rho\ (g/cm^3) \times 4\pi \times 10^{-4}\ (T / (emu/g \cdot g/cm^{-3}))$$

Now, substituting Js into the (BH)max formula:

$$(BH)_{max\_ideal}\ (J/m^3) = [\sigma s \times \rho \times 4\pi \times 10^{-4}]^2 / (4 \times 4\pi \times 10^{-7})$$

$$(BH)_{max\_ideal}\ (J/m^3) = (\sigma s \times \rho)^2 \times (16\pi^2 \times 10^{-8}) / (16\pi \times 10^{-7})$$

$$(BH)_{max\_ideal}\ (J/m^3) = (\sigma s \times \rho)^2 \times \pi \times 10^{-1}$$

To convert J/m³ to kJ/m³.

$$(BH)_{max\_ideal}\ (kJ/m^3) = (\sigma s\ (emu/g) \times \rho\ (g/cm^3))^2 \times \pi \times 10^{-4}$$

To convert kJ/m³ to MGOe (MegaGauss-Oersted):

$$1\ MGOe = 100 / (4\pi)\ kJ/m^3 \approx 7.9577\ kJ/m^3$$

So, $(BH)_{max}$ (MGOe) = $(BH)_{max}$ (kJ/m³) / (100 / (4π)) = $(BH)_{max}$ (kJ/m³) × 0.12566

Example: calculation of $(BH)_{max}$ for Sample A ($SmFe_9Co_2Ti$), 8h milled, annealed at 1123 K for 60 min.

Step 1: Estimate Densities (ρ)

Unit cell parameters a = 0.8557 nm, c = 0.4784 nm. Space group I4/mmm (Z=2 formula units/cell).

Molar Mass ($SmFe_9Co_2Ti$) ≈ 150.36 (Sm) + 9×55.845 (Fe) + 2×58.933 (Co) + 1×47.867 (Ti) ≈ 818.7 g/mol

Volume $V = a^2c = (0.8557\times10^{-9}\ m)^2 \times (0.4784\times10^{-9}\ m) \approx 0.3503 \times 10^{-27}\ m^3$.

$\rho = (Z \times MolarMass) / (V \times AvogadroNo) = (2 \times 818.7) / (0.3503\times10^{-27} \times 6.022\times10^{23}) \approx 1637.4 / 0.21096 \approx 7761\ kg/m^3 = 7.76\ g/cm^3$ (for Sample A-type).

Step 2: Calculations of $(BH)_{max}$ for selected sample

M_{3T} (σ_s) = 105 emu/g or 105 Am²/kg (annealing time 60 min), ρ = 7.76 g/cm³

$(BH)_{max}\ (kJ/m^3) = (105 \times 7.76)^2 \times \pi \times 10^{-4} = (814.8)^2 \times \pi \times 10^{-4} \approx 663903 \times \pi \times 10^{-4} \approx 208.6\ kJ/m^3$

$(BH)_{max}$ (MGOe) = 208.6 × 0.12566 ≈ 26.2 MGOe